THE JOURNAL OF BIOLOGICAL CHEMISTRY VOL. 288, NO. 41, pp. 29736–29745, October 11, 2013

Identification of a Bis-molybdopterin Intermediate in Molybdenum Cofactor Biosynthesis in *Escherichia coli*[*]

Received for publication, July 2, 2013, and in revised form, August 30, 2013 Published, JBC Papers in Press, September 3, 2013, DOI 10.1074/jbc.M113.497453

Stefan Reschke[‡], Kajsa G. V. Sigfridsson[§1], Paul Kaufmann[‡], Nils Leidel[§], Sebastian Horn[§], Klaus Gast[¶], Carola Schulzke[‖2], Michael Haumann[§], and Silke Leimkühler[‡3]

From the [‡]Institute for Biochemistry and Biology, Department of Molecular Enzymology, and the [¶]Institute for Biochemistry and Biology, Department of Physical Biochemistry, University of Potsdam, 14476 Potsdam, Germany, the [§]Institute for Experimental Physics, Free University Berlin, 14195 Berlin, Germany, and the [‖]Institute for Biochemistry, Ernst-Moritz-Arndt University Greifswald, 17487 Greifswald, Germany

Background: Some molybdoenzymes in prokaryotes contain the bis-molybdopterin guanine dinucleotide cofactor.
Results: The bis-Mo-MPT cofactor is a novel intermediate in Moco biosynthesis in *E. coli*.
Conclusion: Bis-MGD formed by MobA is fully functional and restores the catalytic activity in apoTorA.
Significance: Bis-Mo-MPT assembles spontaneously on MobA prior to forming bis-MGD.

The molybdenum cofactor is an important cofactor, and its biosynthesis is essential for many organisms, including humans. Its basic form comprises a single molybdopterin (MPT) unit, which binds a molybdenum ion bearing three oxygen ligands via a dithiolene function, thus forming Mo-MPT. In bacteria, this form is modified to form the bis-MPT guanine dinucleotide cofactor with two MPT units coordinated at one molybdenum atom, which additionally contains GMPs bound to the terminal phosphate group of the MPTs (bis-MGD). The MobA protein catalyzes the nucleotide addition to MPT, but the mechanism of the biosynthesis of the bis-MGD cofactor has remained enigmatic. We have established an *in vitro* system for studying bis-MGD assembly using purified compounds. Quantification of the MPT/molybdenum and molybdenum/phosphorus ratios, time-dependent assays for MPT and MGD detection, and determination of the numbers and lengths of Mo–S and Mo–O bonds by X-ray absorption spectroscopy enabled identification of a novel bis-Mo-MPT intermediate on MobA prior to nucleotide attachment. The addition of Mg-GTP to MobA loaded with bis-Mo-MPT resulted in formation and release of the final bis-MGD product. This cofactor was fully functional and reconstituted the catalytic activity of apo-TMAO reductase (TorA). We propose a reaction sequence for bis-MGD formation, which involves 1) the formation of bis-Mo-MPT, 2) the addition of two GMP units to form bis-MGD on MobA, and 3) the release and transfer of the mature cofactor to the target protein TorA, in a reaction that is supported by the specific chaperone TorD, resulting in an active molybdoenzyme.

The biosynthesis of the molybdenum cofactor (Moco)[4] is an ancient, ubiquitous, and highly conserved pathway leading to the biochemical activation of molybdenum (1). In Moco, the molybdenum atom is coordinated to the dithiolene group of the 6-alkyl side chain of a tricyclic pyranopterin called molybdopterin (MPT) (2). Moco biosynthesis has been studied in detail in *Escherichia coli* by using a combination of biochemical, genetic, and structural approaches (3, 4) and has been divided into four major steps: 1) formation of cyclic pyranopterin monophosphate from 5′-GTP (5, 6), 2) formation of MPT from cyclic pyranopterin monophosphate by insertion of two sulfur atoms (7–10), 3) insertion of molybdenum to form Mo-MPT via an adenylated MPT intermediate (11–13), and 4) additional modification by the covalent addition of GMP or CMP to the C4′ phosphate of MPT via a pyrophosphate bond to form the MPT-guanine or MPT-cytosine dinucleotide cofactors (MGD (14) or MCD (15)), respectively.

After the synthesis of MCD or MGD in *E. coli*, the cofactor can be further modified. In MCD-containing enzymes, like the periplasmic aldehyde oxidoreductase PaoABC (16), the Moco contains an equatorial sulfido ligand at the molybdenum atom, which is essential for the catalytic activity of this class of enzymes (17). For the final step of MGD biosynthesis, two cofactor molecules are ligated to one molybdenum atom, forming the bis-MGD cofactor (18). In *E. coli*, GMP attachment to Mo-MPT is catalyzed by the MobA and MobB proteins, thereby forming MGD (19). MobA is crucial for this reaction and acts as a GTP:molybdopterin guanylyltransferase (14), whereas MobB is not essential (20). The type of Moco and

* This work was supported by the Deutsche Forschungsgemeinschaft (DFG) Cluster of Excellence "Unifying Concepts in Catalysis" (to S. L.), by DFG Grant LE1171/6-1 (to S. L.), and by a Heisenberg Fellowship and Grants Ha3265/3-1 and Ha3265/6-1 from the DFG (to M. H.). This work was also supported by European Cooperation in Science and Technology (COST) Action CM1003 (to S. L. and C. S.).

[1] Recipient of fellowships from "Stiftelsen Bengt Lundqvist minne" and the Wenner-Gren Foundation. Present address: MAX IV Laboratory, Lund University, 22100 Lund, Sweden.

[2] Supported by the European Research Council (ERC).

[3] To whom correspondence should be addressed: Institut für Biochemie und Biologie, Professur für Molekulare Enzymologie, Universität Potsdam, Karl-Lieknecht Strasse 24-25, 14476 Potsdam, Germany. Tel.: 49-331-977-5603; Fax: 49-331-977-5128; E-mail: sleim@uni-potsdam.de.

[4] The abbreviations used are: Moco, molybdenum cofactor; BVS, bond valence sum; EXAFS, extended X-ray absorption fine structure; hSO, human sulfite oxidase; MGD, molybdopterin-guanine dinucleotide; MCD, molybdopterin-cytosine dinucleotide; MPT, molybdopterin; TMAO, trimethylamine *N*-oxide; XANES, X-ray absorption near edge structure; XAS, X-ray absorption spectroscopy.

ligand composition at the molybdenum atom divides the molybdoenzymes of *E. coli* into three families with the following coordination environment: the sulfite oxidase family (dioxo Mo-MPT with a protein cysteinate ligand), the xanthine oxidase family (mono-oxo MCD with a terminal sulfur ligand), and the dimethyl sulfoxide (DMSO) reductase family (bis-MGD with one oxo and one amino acid ligand) (1, 3). Most *E. coli* molybdoenzymes, like the TMAO reductase TorA, belong to the DMSO reductase family and utilize the bis-MGD form of Moco (21). However, it has remained unclear at which stage of Moco biosynthesis the bis-form of the MGD cofactor is built and whether this occurs on MobA or at the respective target enzyme during the insertion process.

It has been shown that MGD was only formed by MobA when the molybdenum atom was already ligated to MPT (22, 23). The crystal structure of MobA has revealed two conserved binding sites, one of which was predicted to bind MPT and the other of which was proposed to bind GTP (24). The MobA enzyme has an overall $\alpha\beta$ architecture, in which the N-terminal domain of the molecule adopts a Rossmann fold (24). From the crystal structure and from previous studies, it is not known so far whether MobA, in addition to MGD formation, also catalyzes the step of the bis-MGD assembly (21).

The last steps of Moco modification, including the formation of bis-MGD, prepare the cofactor for insertion into the specific apoenzymes. The insertion step is catalyzed by Moco-binding molecular chaperones, which bind the respective molybdenum cofactor and insert it into the target molybdoenzyme (25). With a few exceptions, most of the molybdoenzymes have a specific chaperone for Moco insertion. One well studied example is the TorD/TorA system for TMAO reductase in *E. coli*. TorD was shown to be the specific chaperone for TorA (26) and plays a direct role in the insertion of Moco into apoTorA (27). During this reaction, TorD interacts with both MobA and apoTorA and further stabilizes apoTorA for Moco insertion to avoid a proteolytic attack of the latter. This is consistent with its role as "facilitator" of the bis-MGD insertion and maturation of the apoenzyme (21, 25, 28).

In this work, we have established an *in vitro* system for specifically addressing the mechanism for bis-MGD formation. By studies quantifying the metal and cofactor content, in addition to determination of the structure of the molybdenum center by X-ray absorption spectroscopy (XAS), we show that bis-Mo-MPT formation precedes nucleotide addition in the bis-MGD synthesis and that these steps are solely catalyzed by MobA. The detection of the bis-Mo-MPT intermediate is a novel finding for Moco biosynthesis in *E. coli*.

MATERIALS AND METHODS

Expression and Protein Purification—Human sulfite oxidase (hSO) was expressed from plasmid pTG718 (29) in *E. coli* TP1000 (19) cells and purified as described previously (29). The proteins MobA (pCT800A (22)), MoeA (pJNeA11 (30)), and MogA (pMW15gA (31)) were expressed as fusion proteins containing N-terminal His_6 tags in *E. coli* BL21(DE3) cells. After cell lysis, the cleared lysates were applied to 0.75 ml of nickel tris(carboxymethyl)ethylene diamine/liter of culture. The column was washed with 20 column volumes of phosphate buffer containing sequentially 10 and 20 mM imidazole. Proteins were eluted with phosphate buffer containing 250 mM imidazole, dialyzed against 50 mM Tris, 1 mM EDTA, pH 7.5, and stored at −80 °C until further use. ApoTorA (from pJF119EH (27)) and TorD (from pET28TorD (27)) were expressed and purified as described previously but applied to 0.5 ml of nickel nitrilotriacetate resin (Qiagen)/liter of culture. TorD was induced with 0.2 mM L-arabinose as described before (27).

Moco Binding Experiments—MogA, MoeA, and MobA were incubated with Mo-MPT extracted from hSO (29, 32) under anaerobic conditions. Mo-MPT was extracted from aliquots of hSO (240–250 μM) by incubation at 95 °C for 4 min. The supernatant was filtered through Centricon ultrafiltration devices (10 kDa cut-off). The filtered Mo-MPT was added to either 30–40 μM MogA, MoeA, or MobA and incubated for 2 h in a total volume of 7–8 ml. After separation of the protein fractions using G25 columns (PD10, GE Healthcare), the proteins were concentrated to molybdenum contents of 0.5–1 mM for XAS measurements. The binding experiments were performed in the presence or absence of 2.5 mM $MgCl_2$ and 380 μM GTP.

Metal and Cofactor Content Quantification—Molybdenum analysis and quantification of further components in protein samples were performed using inductively coupled plasma optical emission spectroscopy on a PerkinElmer Life Sciences Optima 2100DV instrument as described previously (33) or total reflection X-ray fluorescence analysis (34) on a PicoFox spectrometer (Bruker). By total reflection X-ray fluorescence analysis, molybdenum and phosphorus contents per protein were determined in samples, to which sodium phosphate and/or molybdenum acetate had been added as standards in a concentration series. The respective element concentrations in the protein samples were determined from linear fits to the magnitudes of the elemental K_α X-ray fluorescence of the sample series and extrapolation to the point of zero molybdenum or phosphorus addition (not shown), relative to cesium acetate and gallium elemental standards (Sigma) and relative to the respective protein concentration. MPT contents were determined fluorometrically after conversion of the molecule to form A, as described previously (35). The formation of MGD was assayed fluorometrically after its conversion to form A-GMP (36). The fluorescence of form A and form A-GMP was monitored by an Agilent 1260-series detector using excitation at 383 nm and emission detection at 450 nm.

Time-dependent MGD Formation by MobA—MGD formation as a function of the incubation time was assayed at room temperature in a total sample volume of 200 μl, containing 5 μM MobA, 1 mM $MgCl_2$, 1 mM GTP, 50 μl of supernatant of 300 μM heat-denatured hSO (incubated at 95 °C for 2 min), and 120 μl of 100 mM Tris buffer (pH 7.2).

Bis-MGD Insertion into apoTorA—An *in vitro* assay was used for the insertion of *in vitro* synthesized bis-MGD into apoTorA (26). The assay consisted of apoTorA (1 μM), MobA (0.955 μM), GTP (1 mM), $MgCl_2$ (1 mM), and 200 μl of Mo-MPT filtrate from heat-denatured hSO (250 μM) (29) in a total volume of 300 μl of 100 mM phosphate buffer (pH 6.5) and was incubated at 37 °C under anaerobic conditions. The assay was performed in the presence or absence of TorD (3.74 μM). TorA activity was measured in 3944 μl of 100 mM phosphate buffer (pH 6.5),

containing 20 μl of 1.5 M TMAO, 16 μl of 100 mM benzyl viologen, 30 μl of the incubation mixture and was adjusted with sodium dithionite to an A_{600} of 1.0. The oxidation of reduced benzyl viologen was monitored at 600 nm. The specific TorA activity was defined as the oxidation of 1 μmol of benzyl viologen/min/mg of protein.

XAS—XAS at the molybdenum K-edge was performed at SOLEIL (Paris, France) at the SAMBA beamline as described previously (37), using an Si[220] double-crystal monochromator. The synchrotron was operated at a current of 400 mA in top-up mode. The incident energy axis was calibrated (accuracy ±0.15 eV) using the first inflection point at 20,003.9 eV in the simultaneously measured absorption spectrum of a molybdenum foil as a standard. Fluorescence-detected XAS spectra were measured using energy-resolving 7- or 36-element solid-state germanium detectors (Canberra), which were shielded by 10-μm zirconium foil against scattered incident X-rays. Samples were held in a liquid helium cryostat at 20 K. Dead time-corrected XAS spectra (1–2 scans/sample spot) were averaged (5–10 scans/sample) and normalized, and EXAFS oscillations were extracted as described previously (38). k^3-weighted EXAFS spectra were simulated ($S_0{}^2 = 1.0$) using phase functions calculated with FEFF7 (39). Fourier transforms of EXAFS spectra were calculated using in-house software and $\cos^2$ windows extending over 10% at both k-range ends ($k = 2$–14 Å^{-1}). E_0 was refined to 20,014 ± 2 eV in the fit procedure. The fit quality was judged by calculation of the Fourier-filtered R-factor (R_F) (38). The pre-edge structure of XANES spectra was isolated by subtracting a polynomial spline from the main K-edge rise using the software XANDA (XANES Dactyloscope for Windows, K. V. Klementiev; available on the World Wide Web). K-edge energies reflect values at 50% of normalized edge absorption (edge half-height).

Bond valence sum (BVS) calculations were performed using Equation 1 (41) and N (coordination number) and R (interatomic distance) values derived from EXAFS analysis (the sum is over all Mo–S and Mo–O bonds). The used B value was 0.37. For R_0 values, see the legend to Table 4.

$$BVS = \sum N \exp\left(\frac{R_0 - R}{B}\right) \qquad \text{(Eq. 1)}$$

RESULTS

Characterization of MGD Cofactor Formation by MobA—To analyze the reaction catalyzed by MobA, we made use of an *in vitro* system consisting of purified MobA, Mo-MPT from hSO, $MgCl_2$, and GTP (22). On the basis of this system, MGD formation was quantified fluorimetrically after conversion to its stable fluorescent degradation product form A-GMP (36). Fig. 1 shows that MobA catalyzed the step of MGD formation continuously in the reaction mixture. A saturation was reached after 2 h, due to the limitation of intact Mo-MPT in the incubation mixture. In addition, the reaction was dependent on the presence of $MgCl_2$, as suggested by the Rossman fold of the protein, showing that GTP is only bound and converted as a Mg-GTP complex. However, the results also showed that MGD was produced by MobA under the experimental conditions and

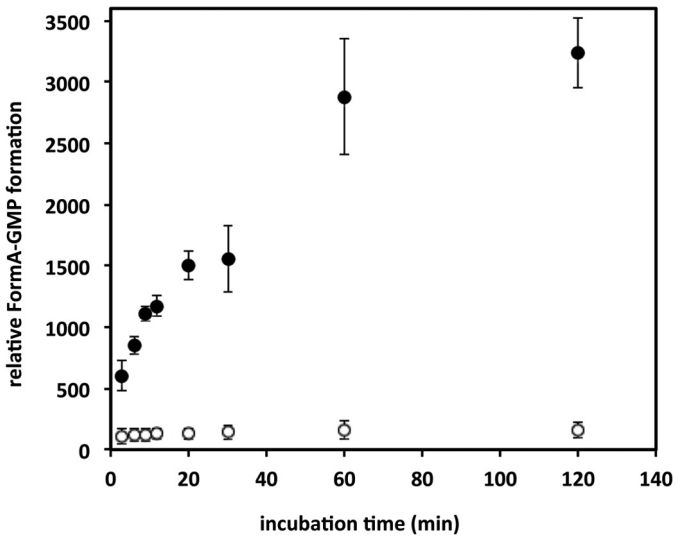

FIGURE 1. **Time-dependent MGD production by MobA.** Incubation mixtures contained 5 μM MobA, Mo-MPT (supernatant of 300 μM heat denatured hSO), and 1 mM GTP, in the absence (*open circles*) or presence (*solid circles*) of $MgCl_2$. MGD production was monitored under anaerobic conditions by quantification of the fluorescence of form A-GMP (36) (excitation at 383 nm and emission at 450 nm) after separation on a reversed phase HPLC column. *Error bars*, S.D.

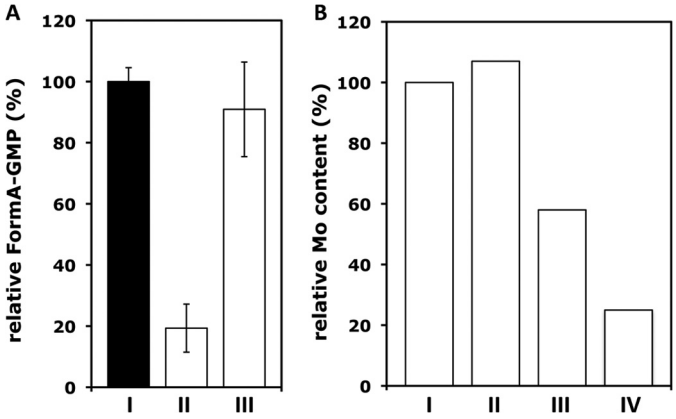

FIGURE 2. **Release of the bis-MGD product from MobA.** *A*, relative form A-GMP contents in reaction mixtures containing 5 μM MobA, Mo-MPT (supernatant of 300 mM hSO, incubated for 2 min at 95 °C), 1 mM GTP, and 1 mM $MgCl_2$ after 2 h of incubation at 37 °C. The form A-GMP content was determined in the total incubation mixture (*I*), in the protein fraction (*II*), and in the respective supernatant (*III*) after separation on a G25 gel filtration column. Total MGD determined was set to 100%. *B*, relative molybdenum contents from assaying the molybdenum K_α X-ray fluorescence intensity at ~17,400 eV (not shown) in samples containing 0.47 μmol of MobA, to which Mo-MPT from hSO had been added and, in addition, no GTP (*I*) or 0.033 μmol (*II*), 4.6 μmol (*III*), or 38 μmol (*IV*) of Mg-GTP. Data were normalized to the molybdenum content of the MobA + Mo-MPT sample without Mg-GTP. *Error bars*, S.D.

that the incubation mixture was suitable to analyze the reaction product of MobA further.

We therefore analyzed whether a portion of MGD remained bound to MobA after the nucleotide addition. MobA was separated from the small molecular weight fraction of the reaction mixture by gel filtration on a desalting column, and the total MGD content was related to MGD that remained bound to MobA or was released to the solution. MGD was quantified after its conversion to form A-GMP (Fig. 2*A*). The purified MobA fraction contained about 19.3 ± 7.9% of the total MGD formed, whereas the majority of MGD (90.9 ± 15.5%) was

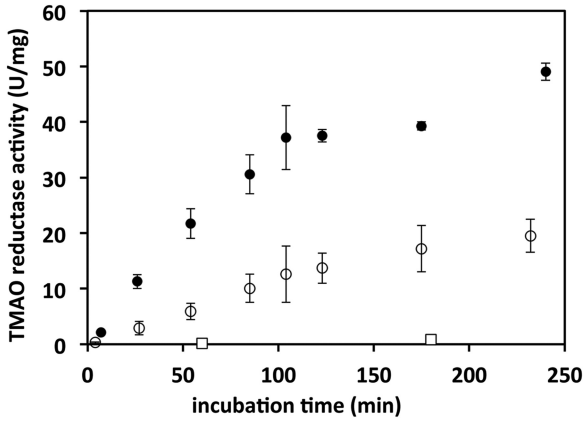

FIGURE 3. **Reconstitution of TMAO reductase activity in apoTorA.** Oxidation of benzyl viologen by TorA was determined at 37 °C under anaerobic conditions. ApoTorA (1 μM), MobA (0.955 μM), GTP (1 mM), and $MgCl_2$ (1 mM) were mixed, and the reconstitution was started by the addition of Mo-MPT, in the presence (*solid circles*) or absence (*open circles*) of 3.74 μM TorD. *Open squares*, incubation mixtures in the absence of MobA. *Error bars*, S.D.

found in the supernatant, showing that the product of MobA was released from the protein.

This result was further corroborated by determination of the relative molybdenum contents by assaying the molybdenum X-ray fluorescence intensity (not shown) in the MobA samples used in the XAS experiments described further below. After the addition of Mg-GTP to MobA, the molybdenum content was decreased to ~50% for a 9-fold excess of GTP and to ~20% for an 80-fold excess of GTP, in comparison with a MobA sample containing only bis-Mo-MPT (Fig. 2*B*). These observations consistently suggest the formation of bis-MGD on MobA in the presence of Mg-GTP and subsequent release of the product from the protein. Additionally, we determined the oligomerization state of MobA during the experiments by dynamic light scattering. The results showed that during the course of the reaction, MobA did not change its oligomerization state and existed as a monomer in solution, also in the incubation mixtures containing Mg-GTP and Mo-MPT (data not shown).

Reconstitution of ApoTorA Using Mo-MPT, Mg-GTP, and MobA—The molybdoenzyme TorA (TMAO reductase from *E. coli*) was used to investigate whether the cofactor produced by MobA was able to reconstitute enzyme activity in the purified apoprotein isolated from a Moco-deficient strain. Purified apoTorA was incubated with MobA, Mo-MPT, GTP, and $MgCl_2$ at 37 °C, and TMAO reductase activity was determined after increasing incubation times of the reaction mixture (Fig. 3). The data showed that the presence of only MobA was sufficient for pronounced activation of apoTorA. No activation was observed in the absence of MobA, showing that other components besides MobA in the reaction mixture were not active in apoTorA activation and that MobA is essential to provide the matured cofactor for TorA, which probably is the bis-MGD cofactor. However, in the presence of the specific Moco-binding chaperone TorD (26), an about 2-fold increase of the maximal TorA activity was observed (Fig. 3). Accordingly, TorD either stabilized the released bis-MGD cofactor synthesized by MobA or facilitated its insertion into apoTorA, thus leading to the higher activity of TorA.

TABLE 1
MPT/molybdenum and phosphorus/molybdenum ratios in different protein samples

Sample	MPT[a]/ Molybdenum[b]	Phosphorus/ Molybdenum[c]
MobA + Mo-MPT	2.18 ± 0.64	2.2 ± 0.7
MobA + Mo-MPT + Mg-GTP	2.28 ± 0.68	3.7 ± 0.8
MoeA + Mo-MPT	0.98 ± 0.06	ND[d]
hSO	1.02 ± 0.03	ND
TorA	ND	3.5 ± 0.6

[a] MPT was detected after conversion to form A.
[b] Molybdenum was quantified by inductively coupled plasma optical emission spectroscopy.
[c] Phosphorus and molybdenum contents were determined by total reflection X-ray fluorescence analysis. The given ratio for MobA + Mo-MPT represents the average of measurements on five independent samples; two samples each for the other conditions were analyzed. The error gives the S.D. MobA + Mo-MPT samples contained 0.67 ± 0.20 mM protein, 0.44 ± 0.18 mM phosphorus, and 0.21 ± 0.09 mM molybdenum on average, consistent with ~30% cofactor loading of MobA. TorA was used at a concentration of 0.42 mM.
[d] ND, not determined.

Quantification of the MPT/Molybdenum and Phosphorus/Molybdenum Ratios on MobA—To get further proof that bis-MGD was formed on MobA, we quantified the MPT/molybdenum ratios in samples containing the MobA protein loaded with Mo-MPT. Samples incubated in the presence or absence of Mg-GTP were compared with those of purified hSO (binding Mo-MPT) and MoeA incubated with Mo-MPT in the same manner (Table 1). An MPT/molybdenum ratio close to 1:1 was found in hSO, consistent with the quantitative presence of the Mo-MPT cofactor in the enzyme. A similar ratio was determined for MoeA incubated with Mo-MPT, supporting previous suggestions that this protein is able to bind exogenously added Mo-MPT (42, 43). These controls emphasized the accuracy of the used method for detection of the MPT/molybdenum ratio.

The MobA protein, which was incubated with Mo-MPT and purified thereafter from the reaction mixture, revealed an MPT/molybdenum ratio close to 2:1, irrespective of the presence or absence of GTP and $MgCl_2$ (Table 1). These results show that, most likely, two MPT units were bound to a single molybdenum ion on MobA, and apparently GTP and $MgCl_2$ were not necessary for the formation of this novel bis-Mo-MPT cofactor precursor. To obtain further proof for the bis-Mo-MPT intermediate, total reflection X-ray fluorescence analysis was used to determine the molybdenum/phosphorus ratios in MobA samples in comparison with the bis-MGD-containing TorA used as a control (Table 1). In samples containing the MobA protein to which Mo-MPT had been previously added, but GTP was absent, a phosphorus/molybdenum ratio close to 2:1 was determined, consistent with one molybdenum and two MPT molecules, which carry one phosphate group each. After the addition of Mo-MPT and Mg-GTP, the phosphorus/molybdenum ratio for MobA was close to 4:1 and is thus similar to the value derived for TorA, which contains the bis-MGD cofactor. This suggested the attachment of two GMP units to the bis-Mo-MPT cofactor on MobA in the presence of Mg-GTP and hence formation of the bis-MGD cofactor (containing four phosphate groups in total).

Determination of Molybdenum Oxidation States and Site Structures by XAS—To further verify the formation of a bis-Mo-MPT intermediate formed on MobA before the Mg-GTP

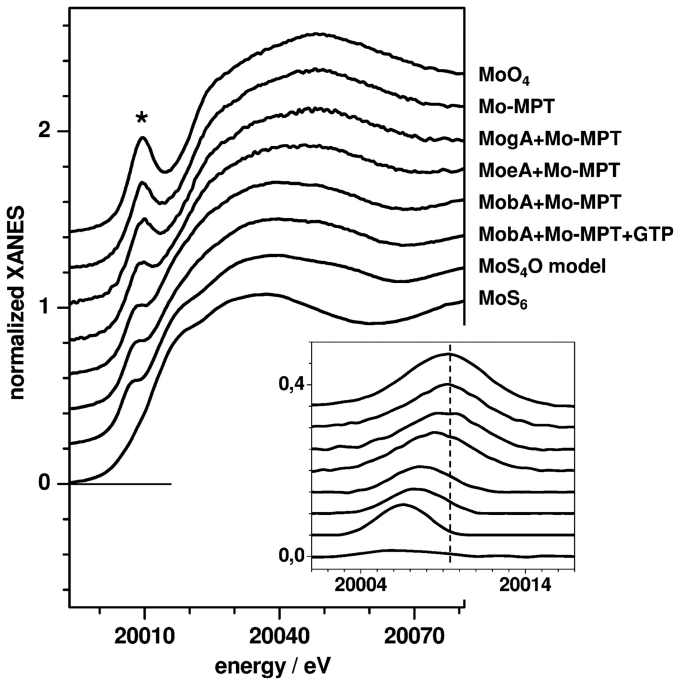

FIGURE 4. **Molybdenum K-edge (XANES) spectra.** The *asterisk* marks the pre-edge features shown in the magnification in the *inset*, after subtraction of the main edge slope. Spectra were vertically displaced for comparison. All protein samples contained Mo-MPT from hSO. *Vertical dashes* in the *inset* denote the pre-edge energy for the molybdate ion. Protein spectra are compared with the following reference compounds. *MoO_4*, $[Mo^{VI}O_4]^{2-}$ ion in 5 mM aqueous solution (pH 7.5); *MoS_4O model*, a synthetic bis-dithiolene complex containing Mo(IV) (see Ref. 45); *MoS_6*, Mo(IV) in solid MoS_2.

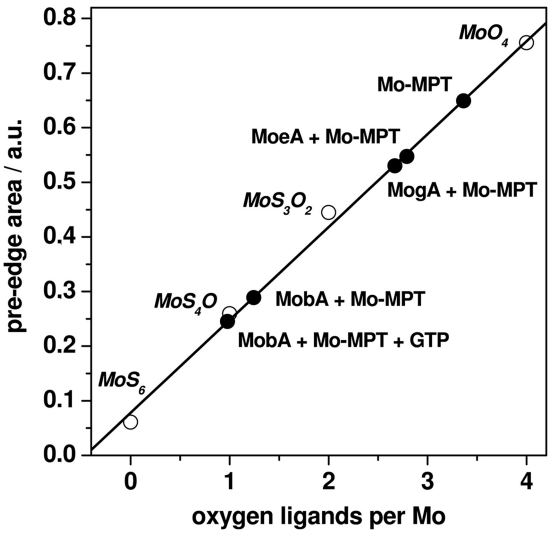

FIGURE 5. **Oxygen ligands per molybdenum from XANES analysis.** Shown are pre-edge areas of the indicated protein samples (*solid circles*) and of the following reference compounds (*open circles*). *MoS_6*, Mo(IV) in solid MoS_2; *MoS_4O*, Mo(IV) in a bis-dithiolene model complex (see Ref. 45); *MoS_3O_2*, Mo(VI) in the Moco in hSO (data not shown); *MoO_4*, Mo(VI) in the aqueous molybdate ion (5 mM, pH 7.5). Pre-edge areas were derived from Gaussian fits (not shown) to data in Fig. 4 (*inset*). The *straight line* represents a fit to the reference data.

addition, XAS experiments were performed to determine the valence state and first-sphere coordination of the molybdenum atom. The coordination of the molybdenum atom was analyzed in samples of MogA, MoeA, or MobA, which were incubated with Mo-MPT in the presence or absence of Mg-GTP. In addition, protein spectra were compared with further reference compounds with known molybdenum coordination. In the hSO enzyme, for example, the molybdenum in the Moco is coordinated by the two sulfurs of the dithiolene moiety of the MPT, two oxygen ligands, and the sulfur from the thiol group of a cysteine residue (MoS_3O_2).

The molybdenum K-edge (XANES) spectrum reflects electronic transitions from the 1*s* core level to unoccupied localized states with mainly metal-*d*/*p* characters (Fig. 4). The main differences in the XANES spectra of the proteins and reference compounds were observed with respect to the amplitude of the pre-edge peak (Fig. 4, *asterisk*). In the case of coordination of molybdenum by oxygen and/or sulfur ligands, this feature is attributable to formally dipole-forbidden 1*s*→4*d* transitions into π^* orbitals oriented along Mo–O bond vectors and thus gains intensity for an increasing number of oxygen ligands (44). The pre-edge peak magnitude therefore was particularly large for the molybdate ion (MoO_4 coordination), decreased for MoS_4O coordination in a synthetic bis-dithiolene model complex (45), and almost absent for MoS_6 coordination in molybdenum disulfide (Fig. 4), revealing a direct dependence of the pre-edge area on the number of oxygen ligands at molybdenum (Fig. 5).

The pre-edge peak areas as determined from the XANES spectra of the protein samples (Fig. 4, *inset*) were compared with the correlation between the pre-edge area and the number of oxygen ligands (Fig. 5). The determined ~3.5 oxygen ligands in the Mo-MPT sample from hSO exceeded the number expected for an $(MPT)S_2MoO_3$ coordination, suggesting an admixture of molybdate of up to ~50%, presumably reflecting oxidatively degraded Moco. The presence of close to 3 oxygen ligands per molybdenum in the MogA + Mo-MPT and MoeA + Mo-MPT samples was in agreement with almost pure $(MPT)S_2MoO_3$ coordination. For MobA + Mo-MPT, a pronounced decrease of the number of oxygen ligands to a value close to unity was observed, irrespective of the presence or absence of Mg-GTP. This indicated the loss of two oxygen ligands at the molybdenum center in the cofactor bound to MobA compared with MoeA.

The position of the K-edge on the incident energy axis is indicative of the metal oxidation state. For various molybdenum reference compounds, the edge energy increased by ~1.2 eV per oxidation state in the range of Mo(IV) to Mo(VI) for varied sulfur/oxygen ligand configuration, but the absolute energies depended on the relative numbers of sulfur and oxygen ligands and were higher by ~5.5 eV for oxygen-only compared with sulfur-only coordination of molybdenum (data not shown). The K-edge energies for the protein samples were determined from the XANES spectra (Fig. 4) and compared with the edge energies of the references (Table 2). The edge energy of the Mo-MPT sample, intermediate between the ones of the $Mo(VI)O_5$ and $Mo(VI)S_2O_3$ species, supports a Mo(VI) oxidation state in the intact cofactor. The value for the MogA + Mo-MPT sample was in agreement with an almost pure $Mo(VI)S_2O_3$ coordination. MoeA + Mo-MPT was located closest to the $Mo(V)S_2O_3$ level. A pronounced edge energy decrease by ~2.5 eV compared with MoeA was observed for MobA + Mo-MPT, both in the absence and presence of Mg-

TABLE 2
Molybdenum K-edge energies and oxidation states

Sample	K-edge energy
	eV
Mo-MPT[a]	20,017.4
MogA + Mo-MPT[a]	20,016.2
MoeA + Mo-MPT[a]	20,015.2
MobA + Mo-MPT[a]	20,013.0
MobA + Mo-MPT + Mg-GTP[a]	20,012.8
$Mo(VI)O_5$[b]	20,018.7
$Mo(VI)S_2O_3$[b]	20,016.3
$Mo(V)S_2O_3$[b]	20,015.1
$Mo(IV)S_4O$[b]	20,012.9

[a] K-edge energies were determined from XANES spectra in Fig. 4.
[b] K-edge energies were determined for molybdenum reference compounds with the indicated metal coordination.

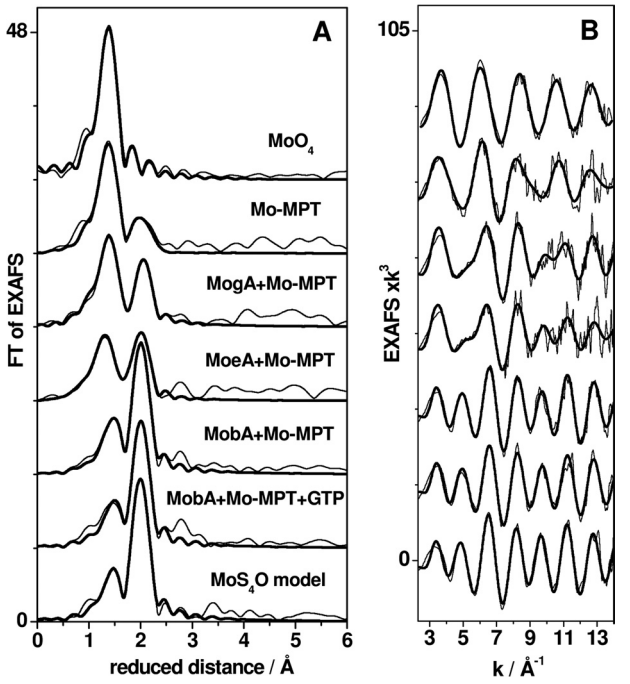

FIGURE 6. **EXAFS analysis of protein samples.** *A*, Fourier transforms (*FT*) of EXAFS oscillations in *B*. *Thin lines*, experimental data; *thick lines*, simulations with parameters in Table 3 (fits 2, 4, 6, 8, 10, 12, and 14). Spectra were vertically displaced for comparison.

GTP (Table 2). This suggests $Mo(V)S_4O$ coordination in MobA (Table 2).

EXAFS analysis was performed to determine the bond lengths and numbers of oxygen and sulfur ligands in the first molybdenum coordination sphere in the protein samples in comparison with selected reference compounds (Fig. 6). Visual inspection of the Fourier transforms in Fig. 6*A* calculated from the EXAFS oscillations in Fig. 6*B* revealed two main Fourier transform peaks for the protein spectra, which are attributable to molybdenum-oxygen (shorter distances) and molybdenum-sulfur (longer distances) bonds, in comparison with the references.

Simulations of the EXAFS spectra yielded the fit parameters listed in Table 3. We show the results of two fit approaches, the first one including only variable fit parameters and the second one using best fit rounded values for the coordination numbers (*N*). The fit results may be summarized as follows, in particular emphasizing the sulfur/oxygen ligand ratios (Table 3). For the Mo-MPT sample, the *N* values for oxygen ligands were higher and for sulfur ligands the values were lower than for a pure MoS_2O_3 coordination. The EXAFS spectra of MogA + Mo-MPT and MoeA + MPT were well described by *N* values, which were close to a pure MoS_2O_3 coordination. However, MoeA + Mo-MPT showed two longer Mo–O^- bonds (~1.8 Å) and one shorter Mo=O bond (~1.7 Å), whereas for MogA + MPT, this was reversed. This is further evidence for the presence of more reduced molybdenum in MoeA. For the MobA + Mo-MPT samples, irrespective of the presence or absence of Mg-GTP, resulting coordination numbers, in comparison with a MoS_4O model complex (45), consistently revealed only one short Mo=O bond and four Mo–S bonds. This clearly indicates the presence of two MPT units bound to molybdenum in MobA. The differences in Mo–S bond lengths of ~0.08 Å suggest that each dithiolene moiety of the two MPT units contributes one longer and one shorter Mo–S bond to the asymmetric ligation at the molybdenum in MobA.

The BVS, as calculated from the molybdenum ligand distances, is a measure of the molybdenum oxidation state (41). BVS values for the protein samples, which were calculated from the distances in Table 3, are summarized in Table 4. The BVS values for the $Mo(VI)O_4$ and $Mo(IV)S_4O$ reference compounds were in good agreement with the known oxidation states. For the Mo-MPT and MogA + Mo-MPT samples, the BVS revealed an oxidation state close to the Mo(VI) level, whereas for MoeA + Mo-MPT, it was closer to Mo(V). For the MobA + Mo-MPT samples, with and without added Mg-GTP, a considerably decreased BVS was in agreement with the predominant presence of Mo(V).

In summary, the XANES and EXAFS analyses provided a consistent picture of the molybdenum oxidation states and coordination environments. Mo-MPT extracted from hSO, which was used for the binding experiments, revealed only a ~50% fraction of intact cofactor. Nonspecific binding of the cofactor to MogA could be used for purification and stabilization of the intact cofactor, in terms of $(MPT)S_2Mo(VI)(=O)_2O^-$ coordination in Mo-MPT. MoeA was also binding only intact Mo-MPT, but this lead to an apparent (partial) reduction of the molybdenum in $(MPT)S_2Mo(V)(=O)(O^-)_2$ sites. The addition of Mo-MPT to MobA produced $S_4Mo(V)(=O)$ species with similar structures both in the absence and presence of added Mg-GTP, thus indicating the formation of bis-Mo-MPT or bis-MGD cofactors solely by MobA.

DISCUSSION

This report describes the formation of a bis-Mo-MPT cofactor, which represents a novel intermediate in Moco biosynthesis in *E. coli*. Our stepwise *in vitro* assay showed that bis-Mo-MPT formation is solely catalyzed by the MobA protein in the presence of Mo-MPT. The formation of bis-Mo-MPT on MobA was unambiguously detected, first, by the MPT/molybdenum ratio of 2:1 and second by the phosphorus/molybdenum ratio of 2:1. Proteins used in comparison showed by X-ray crystallography previously Mo-MPT binding (hSO) (46, 47) or bis-MGD binding (TorA) gave MPT/molybdenum ratios of 1:1 for the former and a phosphorus/molybdenum ratio of 4:1 for the latter enzyme. Third, XAS studies clearly revealed the presence

TABLE 3

Simulation parameters for EXAFS spectra

Simulation parameters describe EXAFS spectra in Fig. 6. *N*, coordination number; *R*, interatomic distance; $2\sigma^2$, Debye-Waller parameter; R_F, error sum as defined in Ref. 38 and calculated for a reduced distance range of 1–2.5 Å.

Sample	Fit no.	Oxygen			Sulfur			R_F
		N (per molybdnum)	*R*	$2\sigma^2 \times 10^3$	*N* (per molybdenum)	*R*	$2\sigma^2 \times 10^3$	
			Å	$Å^2$		Å	$Å^2$	%
MoO_4	1	3.89	1.76	4				12.5
	2	2[a]	1.71	2				11.4
		2[a]	1.77	1				
Mo-MPT	3	3.39	1.75	7	1.68	2.44	9	13.0
	4	2.5[a]	1.72	2	1.5[a]	2.43	8	12.8
		1[a]	1.80	1				
MogA + Mo-MPT	5	2.82	1.76	7	1.90	2.38	5	13.8
	6	2[a]	1.72	3	1[a]	2.34	7	14.1
		1[a]	1.81	2	1[a]	2.39	2	
MoeA + Mo-MPT	7	3.01	1.74	15	2.13	2.37	7	16.2
	8	1[a]	1.72	2	1[a]	2.34	4	8.5
		2[a]	1.81	7	1[a]	2.42	1	
MobA + Mo-MPT	9	1.04	1.71	2	3.88	2.38	7	12.1
	10	1[a]	1.70	2	2[a]	2.31	17	7.2
					2[a]	2.39	2	
MobA + Mo-MPT + Mg-GTP	11	1.14	1.72	4	3.76	2.38	7	13.0
	12	1[a]	1.71	4	2[a]	2.32	23	7.7
					2[a]	2.38	2	
MoS_4O model	13	1.02	1.71	3	4.12	2.39	6	10.3
	14	1[a]	1.72	3	2[a]	2.38	5	9.2
					2[a]	2.48	7	

[a] Parameters that were fixed in the simulation procedures. MoS_4O model denotes a synthetic bis-dithiolene complex (45).

TABLE 4

Bond valence sums from molybdenum-ligand distances

BVS values, which are a measure of the molybdenum oxidation state, were calculated from bond lengths in Table 3 for best fits of EXAFS spectra with rounded coordination numbers, using R_0 values that were the average of values for Mo(IV,V,VI) species (*i.e.* R_0(Mo–O) = 1.878 Å and R_0(Mo–S) = 2.285 Å (40, 41).

Sample	BVS
Mo-MPT	6.09
MogA + Mo-MPT	6.35
MoeA + Mo-MPT	5.51
MobA + Mo-MPT	5.02
MobA + Mo-MPT + Mg-GTP	4.97
Mo(VI)O_4	6.16
Mo(IV)S_4O model	4.15

of four sulfur ligands, from two dithiolene functions, and one Mo=O bond at the molybdenum in MobA, as opposed to only two Mo–S and three Mo–O bonds in the unbound Mo-MPT and in Mo-MPT bound to MoeA and MogA. The proteins MogA and MoeA, which act in the Moco biosynthesis sequence prior to MobA, did not show any activity in bis-Mo-MPT formation. The formation of the bis-Mo-MPT cofactor thus is the first step in the bis-MGD formation catalyzed by MobA.

Only after the addition of Mg-GTP to the bis-Mo-MPT structure on MobA was the final product bis-MGD formed, and the cofactor was released from the protein thereafter. The mature cofactor could be readily inserted into apoTorA, resulting in reconstitution of TMAO reductase activity. This shows that the bis-MGD cofactor formed under our *in vitro* conditions is fully functional and that only MobA is involved in this step. The activity of reconstituted TorA was 2-fold increased in the presence of TorD, which is the specific chaperone for TorA, suggesting either stabilization of bis-MGD in the mixture or facilitation of the insertion process by TorD. The results show that TorD itself is not involved in the bis-MGD formation.

In our study, a Mo-MPT preparation extracted from heat-denatured hSO (29) was used as an effective *in vitro* source for the production of functional bis-MGD by MobA. *In vitro* systems have been used before to insert the cofactor produced by MobA into molybdoenzymes. Moco produced by *E. coli* MobA has been inserted into *Rhodobacter sphaeroides* DMSO reductase (22). Alternatively, *E. coli* TMAO reductase was used to test the activity of MobA in conjunction with TorD using the total extract from *E. coli* cells as a rather undefined Moco source (26). These assay systems thus were intrinsically inhomogeneous, because proteins and/or (non-purified) cofactors from different organisms were used. In our present system, only enzymes from *E. coli* were employed. In addition, a defined Mo-MPT source from hSO was used, which proved to be more effective, because reconstitution of TMAO reductase required less incubation time as compared with the system using DMSO reductase. Inclusion of TorD in the incubation mixture resulted in a 2-fold higher rate of reconstitution and of the maximum activity; thus, TorD accelerates bis-MGD insertion 2-fold and additionally acts as a stabilizing protein for TorA and bis-MGD in this reaction, as proposed before (26).

The molecular mechanism of bis-Mo-MPT formation and its binding mode to MobA, however, need further consideration. Presumably, one molecule of molybdate is released during the combination of two Mo-MPT molecules to form the bis-Mo-MPT cofactor, but the underlying chemistry remains elusive. It also remains possible that MobA binds one Mo-MPT molecule and one MPT molecule from which the bis-Mo-MPT could be formed. Crystal structures have shown either a monomeric (48) or an octameric (24) organization of MobA in the crystals. We have studied the oligomerization state of MobA using analytical gel filtration or dynamic light scattering techniques, which revealed that MobA was present as a monomer in solution under all tested conditions, including the presence of Mo-MPT and Mg-GTP and high protein concentrations. Accordingly, bis-Mo-MPT formation from two Mo-MPT/MPT molecules in solution may occur on monomeric MobA using the MPT and predicted GTP binding sites.

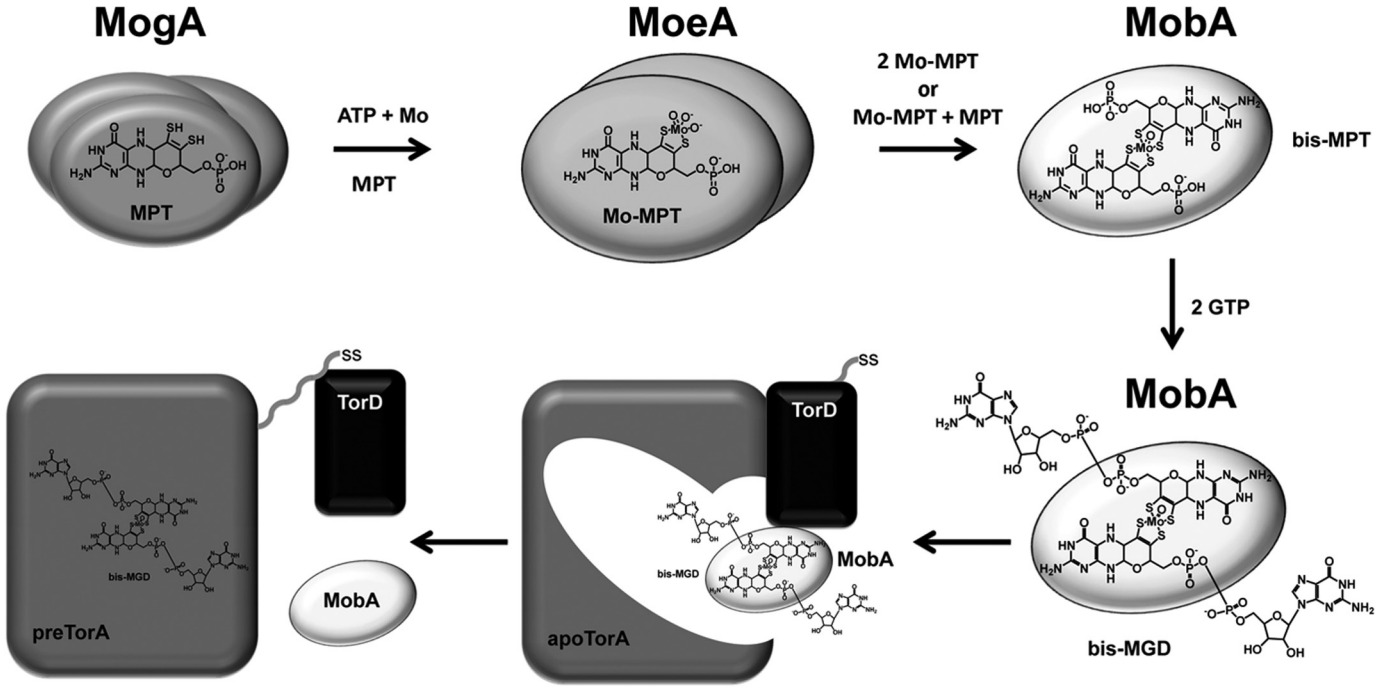

FIGURE 7. **Proposed reaction sequence for bis-MGD formation from bis-Mo-MPT and the involvement of MogA, MoeA, MobA, and TorD in the reconstitution of catalytic activity in apoTorA.** Details are given under "Discussion." *SS*, TAT signal sequence

Here we observed facilitated release of bis-MGD from MobA in the presence of GTP, which could suggest release of the product by competition of GTP with the same site occupied by an MPT unit. Binding of GTP and MPT to the same site may indeed occur, because MPT is derived from GTP in a reaction catalyzed by the MoaA protein (6). Based on these results, we propose that two MPT moieties bind to both the predicted GTP-binding site and the predicted MPT binding site, thus enabling bis-Mo-MPT and bis-MGD synthesis by monomeric MobA. The favorable release only of the final product may then be induced by a different binding mode of bis-MGD compared with bis-Mo-MPT to MobA.

In our *in vitro* system, the formation of bis-MGD readily occurred after the addition of Mg-GTP to MobA loaded with bis-Mo-MPT. *In vivo*, however, MobB, a GTP-binding protein interacting with MobA (20, 49), may assist the GTP binding step. A docking model of MobA and MobB has suggested that GTP is bound to a shared binding site at the interface between both proteins (20). However, MobB did not enhance the activity of MGD formation under our assay conditions (data not shown). In the cell, MobB may deliver GTP to MobA with a high specific affinity in a reaction, which was not required in our *in vitro* assay due to the higher concentrations of GTP. The mature bis-MGD cofactor after its release from MobA is captured by Moco-binding chaperones like TorD, TorZ, NarJ, DmsD, FdhD, or NarW (21). These chaperones assist bis-MGD insertion into the respective target proteins. This has been studied in detail for the TorA/TorD system (25, 28), revealing that a complex comprising the TorA, MobA, and TorD proteins is involved (28).

Based on our present findings and the earlier results, we propose the following sequence of events during bis-MGD biosynthesis for TorA activation in *E. coli* (Fig. 7). 1) MogA forms an MPT-AMP intermediate from MPT and ATP. 2) MoeA takes over the product, inserts the molybdenum ion derived from molybdate in a Zn^{2+}-dependent reaction, and detaches the AMP to form Mo-MPT (43). The MoeA reaction may involve reduction of molybdenum to the Mo(V) level, and the short molybdenum-oxygen bond lengths of the (MPT)MoS_2O_3 site suggest that no amino acid-derived metal ligands are involved in the Mo-MPT binding to MoeA. 3) Mo-MPT is then captured by MobA, which first forms the bis-Mo-MPT cofactor and thereafter attaches two GMP molecules in a GTP- and $MgCl_2$-dependent reaction, producing bis-MGD. MobA-bound bis-Mo-MPT and bis-MGD seemingly contained Mo(V), and the MoS_4O coordination suggests that amino acids are not ligating the molybdenum of either cofactor. 4) TorD then is involved in channeling bis-MGD to apoTorA, and MobA and TorD are released from the complex, resulting in cofactor-loaded enzyme (pre-TorA) (25). 5) Pre-TorA is translocated to the periplasm, where active TorA enzyme is finally generated (21).

Acknowledgments—We thank Chantal Iobbi-Nivol for providing plasmid for expression of TorA and TorD, K. V. Rajagopalan for helpful discussions, and Martin Mahro for help with modeling studies of MobA with Moco.

REFERENCES

1. Hille, R. (1996) The mononuclear molybdenum enzymes. *Chem. Rev.* **96,** 2757–2816
2. Rajagopalan, K. V., and Johnson, J. L. (1992) The pterin molybdenum cofactors. *J. Biol. Chem.* **267,** 10199–10202
3. Rajagopalan, K. V. (1996) Biosynthesis of the molybdenum cofactor. in *Escherichia coli and Salmonella*: *Cellular and Molecular Biology*, Vol. I (Neidhardt, F. C., ed) pp. 674–679, American Society for Microbiology Press, Washington, D. C.
4. Leimkühler, S., Wuebbens, M. M., and Rajagopalan, K. V. (2011) The

history of the discovery of the molybdenum cofactor and novel aspects of its biosynthesis in bacteria. *Coord. Chem. Rev.* **255,** 1129–1144
5. Hänzelmann, P., and Schindelin, H. (2004) Crystal structure of the *S*-adenosylmethionine-dependent enzyme MoaA and its implications for molybdenum cofactor deficiency in humans. *Proc. Natl. Acad. Sci. U.S.A.* **101,** 12870–12875
6. Hover, B. M., Loksztejn, A., Ribeiro, A. A., and Yokoyama, K. (2013) Identification of a cyclic nucleotide as a cryptic intermediate in molybdenum cofactor biosynthesis. *J. Am. Chem. Soc.* **135,** 7019–7032
7. Pitterle, D. M., Johnson, J. L., and Rajagopalan, K. V. (1993) *In vitro* synthesis of molybdopterin from precursor Z using purified converting factor. Role of protein-bound sulfur in formation of the dithiolene. *J. Biol. Chem.* **268,** 13506–13509
8. Gutzke, G., Fischer, B., Mendel, R. R., and Schwarz, G. (2001) Thiocarboxylation of molybdopterin synthase provides evidence for the mechanism of dithiolene formation in metal-binding pterins. *J. Biol. Chem.* **276,** 36268–36274
9. Rudolph, M. J., Wuebbens, M. M., Turque, O., Rajagopalan, K. V., and Schindelin, H. (2003) Structural studies of molybdopterin synthase provide insights into its catalytic mechanism. *J. Biol. Chem.* **278,** 14514–14522
10. Wuebbens, M. M., and Rajagopalan, K. V. (2003) Mechanistic and mutational studies of *Escherichia coli* molybdopterin synthase clarify the final step of molybdopterin biosynthesis. *J. Biol. Chem.* **278,** 14523–14532
11. Joshi, M. S., Johnson, J. L., and Rajagopalan, K. V. (1996) Molybdenum cofactor biosynthesis in *Escherichia coli mod* and *mog* mutants. *J. Bacteriol.* **178,** 4310–4312
12. Kuper, J., Winking, J., Hecht, H. J., Mendel, R. R., and Schwarz, G. (2003) The active site of the molybdenum cofactor biosynthestic protein domain Cnx1G. *Arch. Biochem. Biophys* **411,** 36–46
13. Llamas, A., Mendel, R. R., and Schwarz, G. (2004) Synthesis of adenylated molybdopterin. An essential step for molybdenum insertion. *J. Biol. Chem.* **279,** 55241–55246
14. Palmer, T., Vasishta, A., Whitty, P. W., and Boxer, D. H. (1994) Isolation of protein FA, a product of the *mob* locus required for molybdenum cofactor biosynthesis in *Escherichia coli*. *Eur. J. Biochem.* **222,** 687–692
15. Neumann, M., Mittelstädt, G., Seduk, F., Iobbi-Nivol, C., and Leimkühler, S. (2009) MocA is a specific cytidylyltransferase involved in molybdopterin cytosine dinucleotide biosynthesis in *Escherichia coli*. *J. Biol. Chem.* **284,** 21891–21898
16. Neumann, M., Mittelstädt, G., Iobbi-Nivol, C., Saggu, M., Lendzian, F., Hildebrandt, P., and Leimkühler, S. (2009) A periplasmic aldehyde oxidoreductase represents the first molybdopterin cytosine dinucleotide cofactor containing molybdo-flavoenzyme from *Escherichia coli*. *FEBS J.* **276,** 2762–2774
17. Neumann, M., and Leimkühler, S. (2011) The role of system-specific molecular chaperones in the maturation of molybdoenzymes in bacteria. *Biochem. Res. Int.* 2011, 850924
18. Hilton, J. C., and Rajagopalan, K. V. (1996) Identification of the molybdenum cofactor of dimethyl sulfoxide reductase from *Rhodobacter sphaeroides* f. sp. *denitrificans* as bis(molybdopterin guanine dinucleotide)molybdenum. *Arch. Biochem. Biophys.* **325,** 139–143
19. Palmer, T., Santini, C. L., Iobbi-Nivol, C., Eaves, D. J., Boxer, D. H., and Giordano, G. (1996) Involvement of the *narJ* and *mob* gene products in the biosynthesis of the molybdoenzyme nitrate reductase in *Escherichia coli*. *Mol. Microbiol.* **20,** 875–884
20. McLuskey, K., Harrison, J. A., Schuttelkopf, A. W., Boxer, D. H., and Hunter, W. N. (2003) Insight into the role of *Escherichia coli* MobB in molybdenum cofactor biosynthesis based on the high resolution crystal structure. *J. Biol. Chem.* **278,** 23706–23713
21. Iobbi-Nivol, C., and Leimkühler, S. (2013) Molybdenum enzymes, their maturation and molybdenum cofactor biosynthesis in *Escherichia coli*. *Biochim. Biophys. Acta* **1827,** 1086–1101
22. Temple, C. A., and Rajagopalan, K. V. (2000) Mechanism of assembly of the bis(molybdopterin guanine dinucleotide)molybdenum cofactor in *Rhodobacter sphaeroides* dimethyl sulfoxide reductase. *J. Biol. Chem.* **275,** 40202–40210
23. Neumann, M., Seduk, F., Iobbi-Nivol, C., and Leimkühler, S. (2011) Molybdopterin dinucleotide biosynthesis in *Escherichia coli*. Identification of amino acid residues of molybdopterin dinucleotide transferases that determine specificity for binding of guanine or cytosine nucleotides. *J. Biol. Chem.* **286,** 1400–1408
24. Lake, M. W., Temple, C. A., Rajagopalan, K. V., and Schindelin, H. (2000) The crystal structure of the *Escherichia coli* MobA protein provides insight into molybdopterin guanine dinucleotide biosynthesis. *J. Biol. Chem.* **275,** 40211–40217
25. Genest, O., Méjean, V., and Iobbi-Nivol, C. (2009) Multiple roles of TorD-like chaperones in the biogenesis of molybdoenzymes. *FEMS Microbiol. Lett.* **297,** 1–9
26. Genest, O., Ilbert, M., Méjean, V., and Iobbi-Nivol, C. (2005) TorD, an essential chaperone for TorA molybdoenzyme maturation at high temperature. *J. Biol. Chem.* **280,** 15644–15648
27. Genest, O., Seduk, F., Théraulaz, L., Méjean, V., and Iobbi-Nivol, C. (2006) Chaperone protection of immature molybdoenzyme during molybdenum cofactor limitation. *FEMS Microbiol. Lett.* **265,** 51–55
28. Genest, O., Neumann, M., Seduk, F., Stöcklein, W., Méjean, V., Leimkühler, S., and Iobbi-Nivol, C. (2008) Dedicated metallochaperone connects apoenzyme and molybdenum cofactor biosynthesis components. *J. Biol. Chem.* **283,** 21433–21440
29. Temple, C. A., Graf, T. N., and Rajagopalan, K. V. (2000) Optimization of expression of human sulfite oxidase and its molybdenum domain. *Arch. Biochem. Biophys.* **383,** 281–287
30. Xiang, S., Nichols, J., Rajagopalan, K. V., and Schindelin, H. (2001) The crystal structure of *Escherichia coli* MoeA and its relationship to the multifunctional protein gephyrin. *Structure* **9,** 299–310
31. Liu, M. T., Wuebbens, M. M., Rajagopalan, K. V., and Schindelin, H. (2000) Crystal structure of the gephyrin-related molybdenum cofactor biosynthesis protein MogA from *Escherichia coli*. *J. Biol. Chem.* **275,** 1814–1822
32. Neumann, M., Schulte, M., Jünemann, N., Stöcklein, W., and Leimkühler, S. (2006) *Rhodobacter capsulatus* XdhC is involved in molybdenum cofactor binding and insertion into xanthine dehydrogenase. *J. Biol. Chem.* **281,** 15701–15708
33. Neumann, M., and Leimkühler, S. (2008) Heavy metal ions inhibit molybdoenzyme activity by binding to the dithiolene moiety of molybdopterin in *Escherichia coli*. *FEBS J.* **275,** 5678–5689
34. Klockenkämper R (1996) *Total Reflection X-ray Fluorescence Analysis* Wiley-VCH, London, UK
35. Johnson, J. L., Hainline, B. E., Rajagopalan, K. V., and Arison, B. H. (1984) The pterin component of the molybdenum cofactor. Structural characterization of two fluorescent derivatives. *J. Biol. Chem.* **259,** 5414–5422
36. Johnson, J. L., Bastian, N. R., and Rajagopalan, K. V. (1990) Molybdopterin guanine dinucleotide. A modified form of molybdopterin identified in the molybdenum cofactor of dimethyl sulfoxide reductase from *Rhodobacter sphaeroides* forma specialis *denitrificans*. *Proc. Natl. Acad. Sci. U.S.A.* **87,** 3190–3194
37. Havelius, K. G., Reschke, S., Horn, S., Döring, A., Niks, D., Hille, R., Schulzke, C., Leimkühler, S., and Haumann, M. (2011) Structure of the molybdenum site in YedY, a sulfite oxidase homologue from *Escherichia coli*. *Inorg. Chem.* **50,** 741–748
38. Dau, H., Liebisch, P., and Haumann, M. (2003) X-ray absorption spectroscopy to analyze nuclear geometry and electronic structure of biological metal centers. Potential and questions examined with special focus on the tetra-nuclear manganese complex of oxygenic photosynthesis. *Anal. Bioanal. Chem.* **376,** 562–583
39. Zabinsky, S. I., Rehr, J. J., Ankudinov, A., Albers, R. C., and Eller, M. J. (1995) Multiple-scattering calculations of X-ray-absorption spectra. *Phys. Rev. B* **52,** 2995–3009
40. Chen, M., Zhou, Z., and Hu, S. (2002) Bond valence parameters linearly dependent on the molybdenum oxidation states. *Chin. Sci. Bull.* **47,** 978–981
41. Liu, W. T., and Thorp, H. H. (1993) Bond valence sum analysis of metal-ligand bond lengths in metalloenzymes and model complexes. 2. Refined distances and other enzymes. *Inorg. Chem.* **32,** 4102–4105
42. Nichols, J., and Rajagopalan, K. V. (2002) *Escherichia coli* MoeA and MogA. Function in metal incorporation step of molybdenum cofactor biosynthesis. *J. Biol. Chem.* **277,** 24995–25000

43. Nichols, J. D., and Rajagopalan, K. V. (2005) *In vitro* molybdenum ligation to molybdopterin using purified components. *J. Biol. Chem.* **280,** 7817–7822
44. Qiu, J. A., Wilson, H. L., Pushie, M. J., Kisker, C., George, G. N., and Rajagopalan, K. V. (2010) The structures of the C185S and C185A mutants of sulfite oxidase reveal rearrangement of the active site. *Biochemistry* **49,** 3989 – 4000
45. Samuel, P. P., Horn, S., Döring, A., Havelius, K. G. V., Reschke, S., Leimkühler, S., Haumann, M., and Schulzke, C. (2011) A crystallographic and Mo K-edge XAS study of molybdenum oxo bis-, mono-, and non-dithiolene complexes. First-sphere coordination geometry and noninnocence of ligands. *Eur. J. Inorg. Chem.* **28,** 4387 – 4399
46. Kisker, C., Schindelin, H., Pacheco, A., Wehbi, W. A., Garrett, R. M., Rajagopalan, K. V., Enemark, J. H., and Rees, D. C. (1997) Molecular basis of sulfite oxidase deficiency from the structure of sulfite oxidase. *Cell* **91,** 973–983
47. Kisker, C., Schindelin, H., and Rees, D. C. (1997) Molybdenum-cofactor-containing enzymes. Structure and mechanism. *Annu. Rev. Biochem.* **66,** 233–267
48. Stevenson, C. E., Sargent, F., Buchanan, G., Palmer, T., and Lawson, D. M. (2000) Crystal structure of the molybdenum cofactor biosynthesis protein MobA from *Escherichia coli* at near-atomic resolution. *Structure* **8,** 1115–1125
49. Magalon, A., Frixon, C., Pommier, J., Giordano, G., and Blasco, F. (2002) *In vivo* interactions between gene products involved in the final stages of molybdenum cofactor biosynthesis in *Escherichia coli*. *J. Biol. Chem.* **277,** 48199 – 48204